Electrodisintegration of ^{16}O and determination of astrophysical S-factors of the inverse reaction

Ivica Friščić

27 May 2022

New Scientific Opportunities with the TRIUMF ARIEL e-linac

University
of Zagreb

Modeling of stellar evolution

- Complicated part: transport of a material inside a star

- Easy part: nucleosynthesis of a burning stage is described by a system of differential equations which are very easy to solve

-> nuclear input enters in form of reaction rates at E_G

-> $^{12}C(\alpha, \gamma)^{16}O$ has the largest uncertainty compared to other rates

-> with triple-alpha reaction part of He-burning stage

-> affects C/O abundance, subsequent nucleosynthesis and end of live of massive stars

Example: R. Farmer et al., 2020 ApJL 902 L36

- Evolution of He-core in mass range between 30 and 200 $M_\odot$ and $^{12}C(\alpha, \gamma)^{16}O$ rate in $\pm 3\sigma_{C12}$ range
- Steps: 1 $M_\odot$ and 0.5 σ_{C12} -> 2210 simulations
- For He-core > 40 $M_\odot$ gamma rays can produce e^-e^+ pairs, radiation pressure drops, leading to gravitational collapse

-> CC – core collapse stars

-> PISN – pair instability supernovae

-> PPISN – pulsational pair instability supernovae

- Using LIGO/Virgo gravitational wave data from binary black hole mergers to determine their masses and subsequently $^{12}C(\alpha, \gamma)^{16}O$ rate

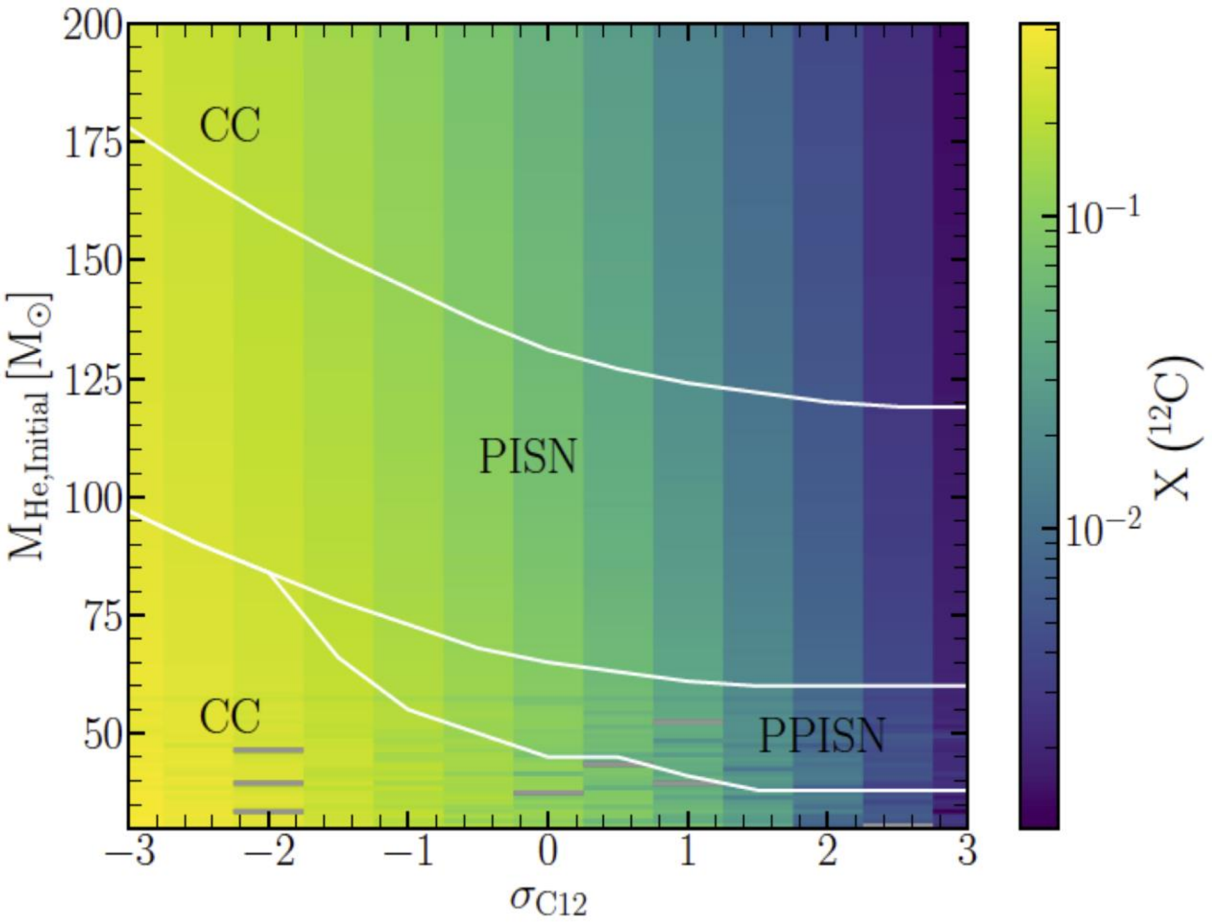

Constraints on $^{12}C(\alpha, \gamma)^{16}O$ S-Factor

galactic chemical enrichment model

observations of white dwarfs

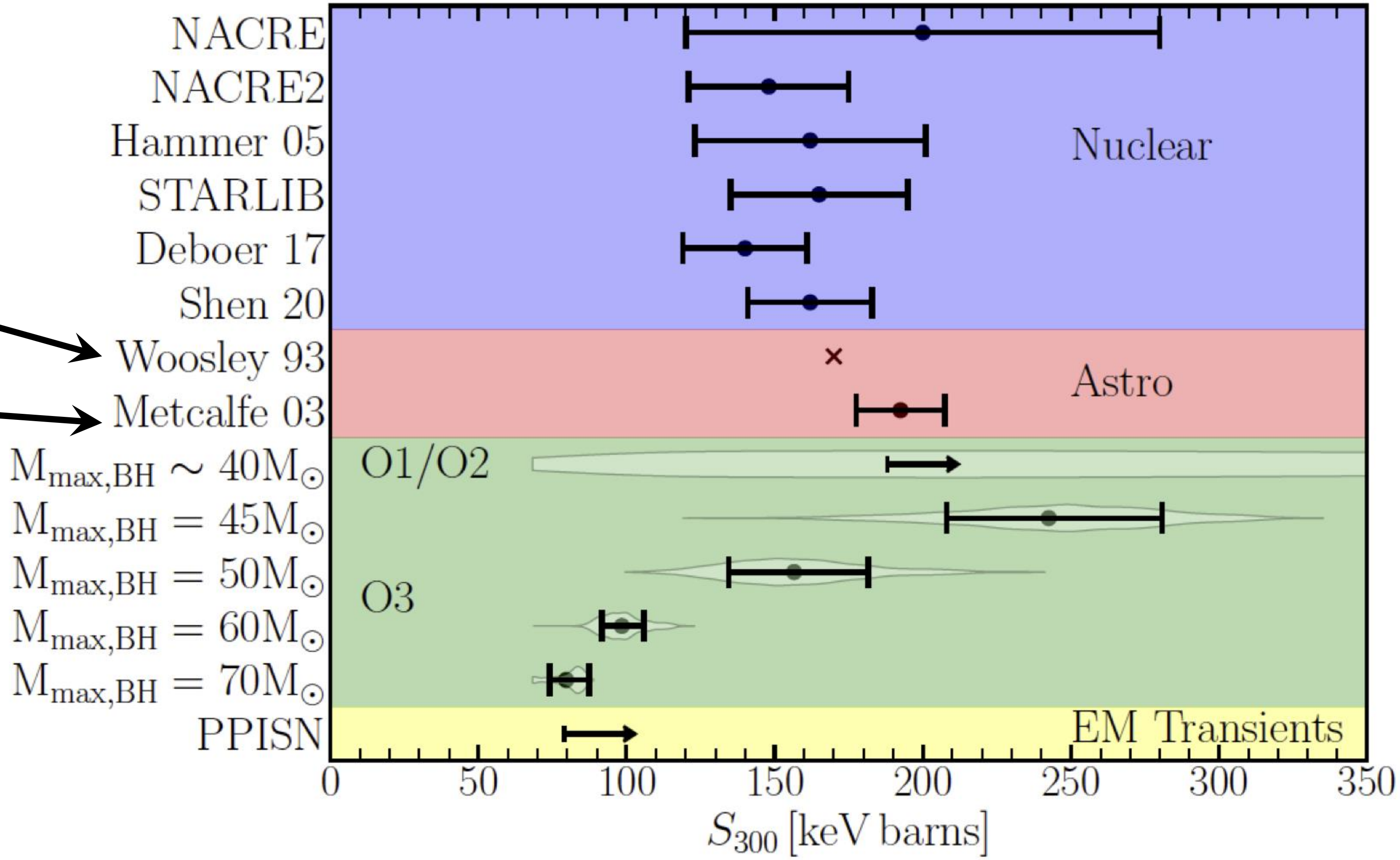

Fig 7. from R. Farmer et al., 2020 ApJL 902 L36

The cross section of $^{12}C(\alpha, \gamma)^{16}O$ at E_G

- $\sigma \simeq 10^{-5}$ pb, due to large Coulomb barrier direct measurement would not feasible
- The cross section at E_G is dominated by two components:

→ E1 component, $J^{\pi} = 1^{-}$: subthreshold state at 7.117 MeV and broad resonance at 9.59 MeV

→ E2 component, $J^{\pi} = 2^{+}$: subthreshold state at 6.917 MeV and narrow resonance at 9.85 MeV

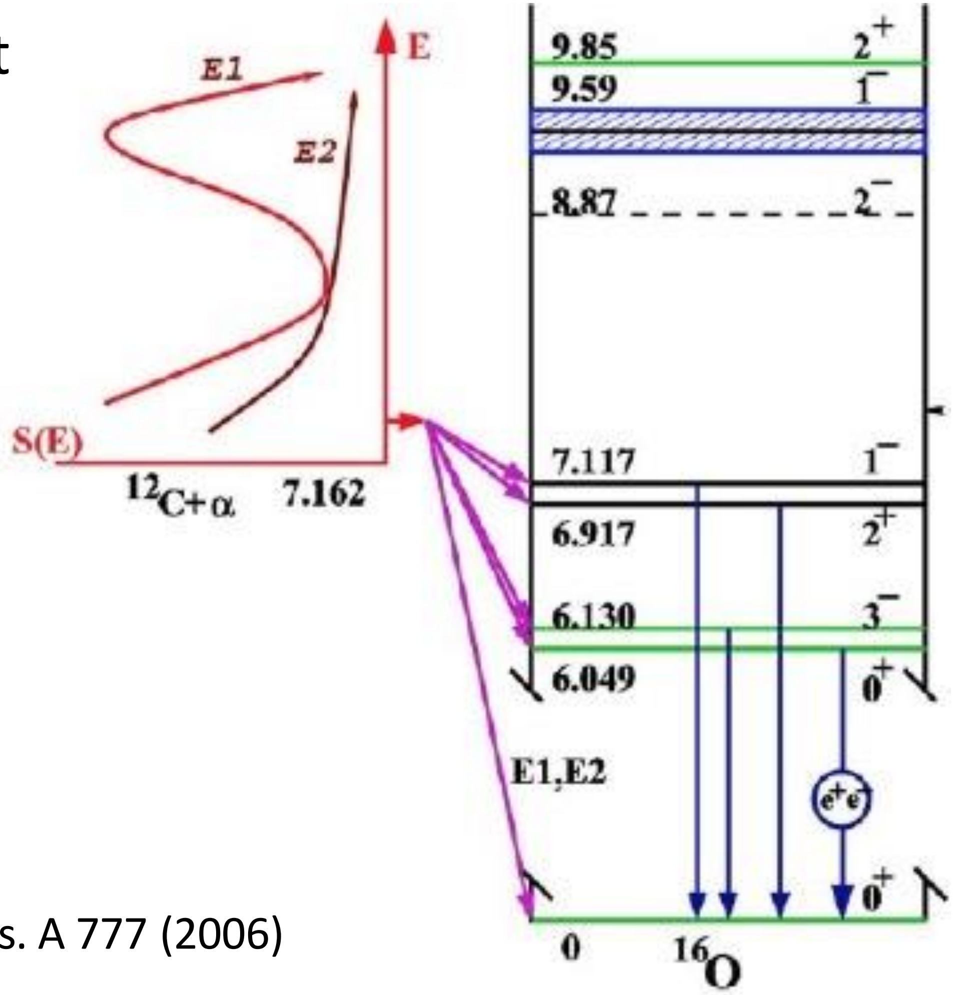

L.R. Buchmann, C.A. Barnes, Nucl. Phys. A 777 (2006)

$^{12}C(\alpha, \gamma)^{16}O$ S-factors components

$$\sigma(E) = \frac{S(E)}{E} e^{-2\pi\eta}$$

$$\eta = \frac{2\pi Z_1 Z_2 e^2}{h v_{rel}}$$

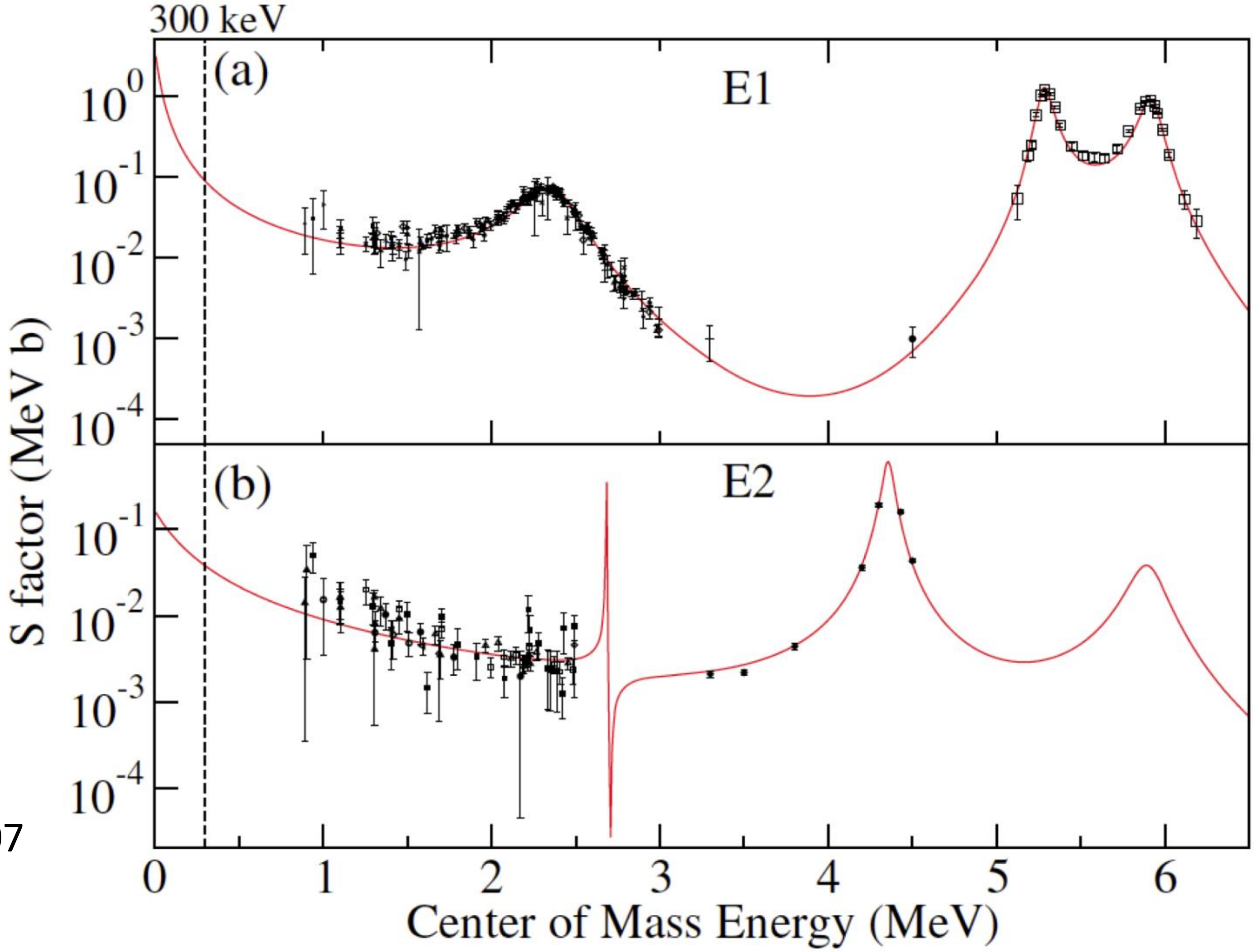

R. J. deBoer et al., Rev. Mod. Phys. 89, 035007 (2017) and references therein

Nuclear measurements

Direct measurements	Indirect measurements
^{12}C(α, γ)^{16}O; α beam: detection of angular distribution of γ; → **S_{E1}** and **S_{E2}**	**β decay of ^{16}N**: $^{16}O^{*}$ → α + ^{12}C; → **S_{E1}**
α(^{12}C,^{16}O) γ; ^{12}C beam (inverse kinematic): detection of ^{16}O recoils; → **S_{tot}**	**Inverse reaction**

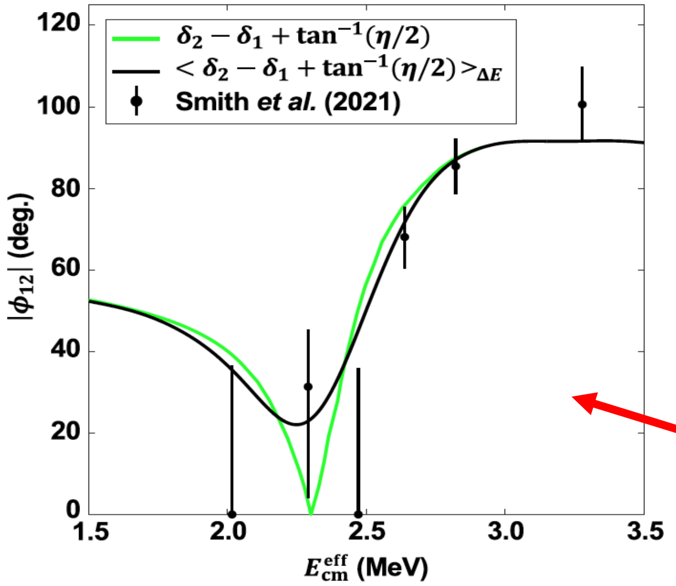

Photodisintegration of ^{16}O: ^{16}O(γ, α)^{12}C	**Electrodisintegration of ^{16}O: ^{16}O(e, e'α)^{12}C**
Bubble chamber, R. J. Holt et al., (2018), arXiv:1809.10176 **Time projection chamber**, M. Gai et al., JINST 5, P12004 (2010), **R. Smith et al., Nat. Commun. 12, 5920 (2021)**	**I. F., W. T. Donnelly and R. G. Milner, Phys. Rev. C 100, (2019) 025804** **S. Lunkenheimer, PhD Thesis 2022, University of Mainz, Germany, MAGIX @Mainz**

Advantage of $^{16}O(e,e'\alpha)^{12}C$

- Inverse reaction: larger cross section than direct reaction
- New generation of energy recovery linear (ERL) accelerators with I ≥ 10 mA (MESA @Mainz, CBETA @Cornell) + oxygen cluster gas-jet target with thickness > 10^{18} atoms/cm^2 (MAGIX @Mainz)

  => Luminosity > 10^{35} 1/(cm^2 s)

- Reaction involves virtual photon exchange

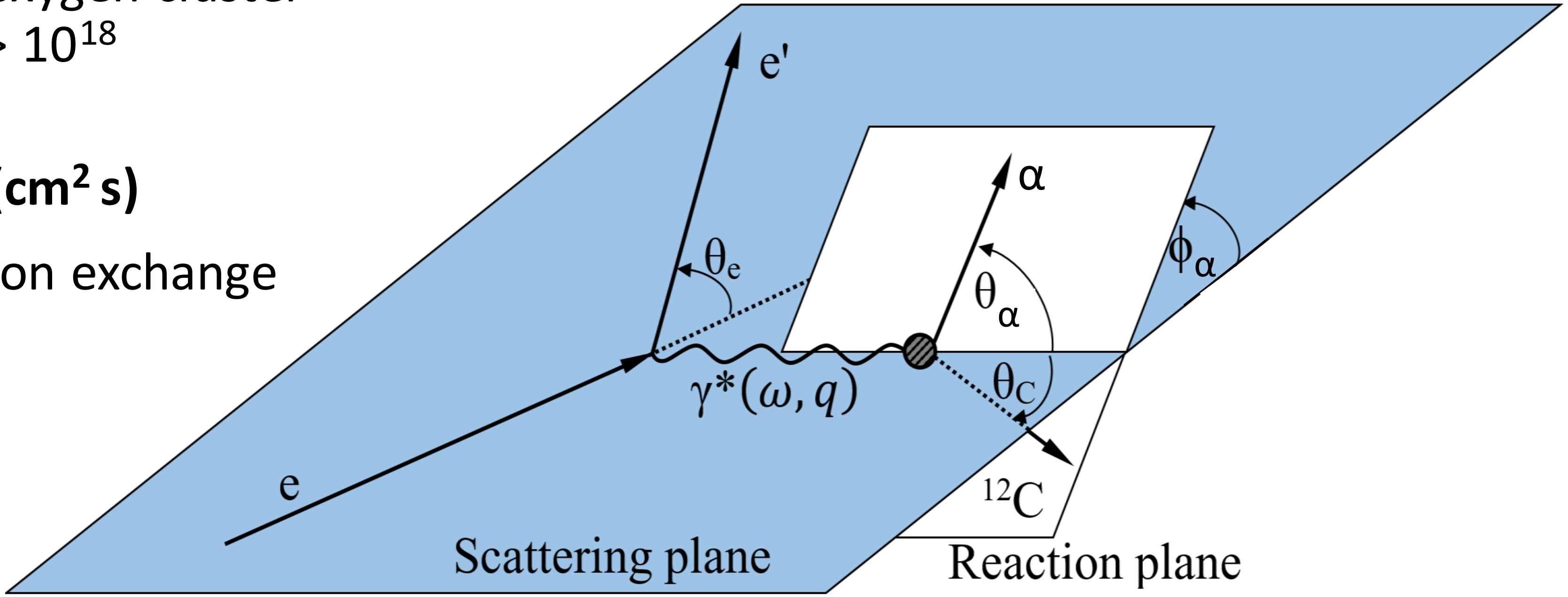

Schematic layout of the ideal experiment

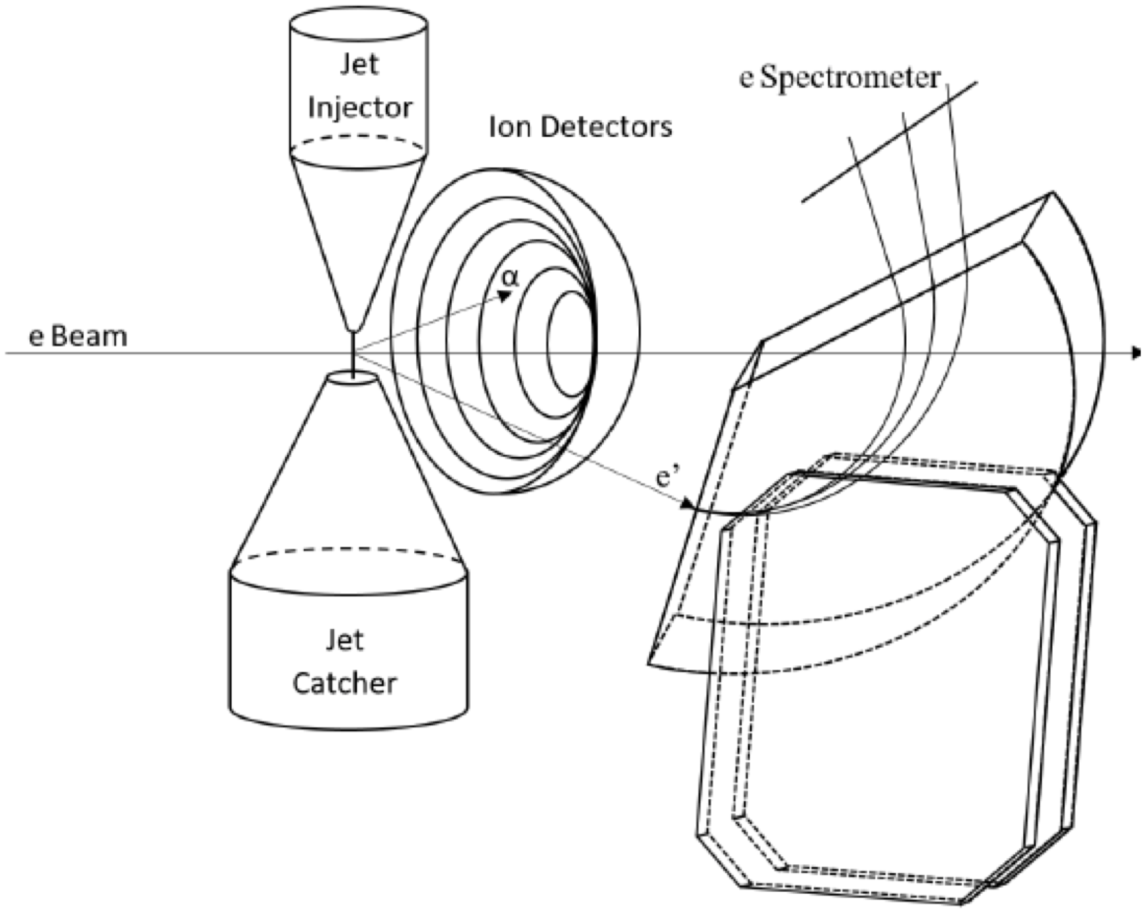

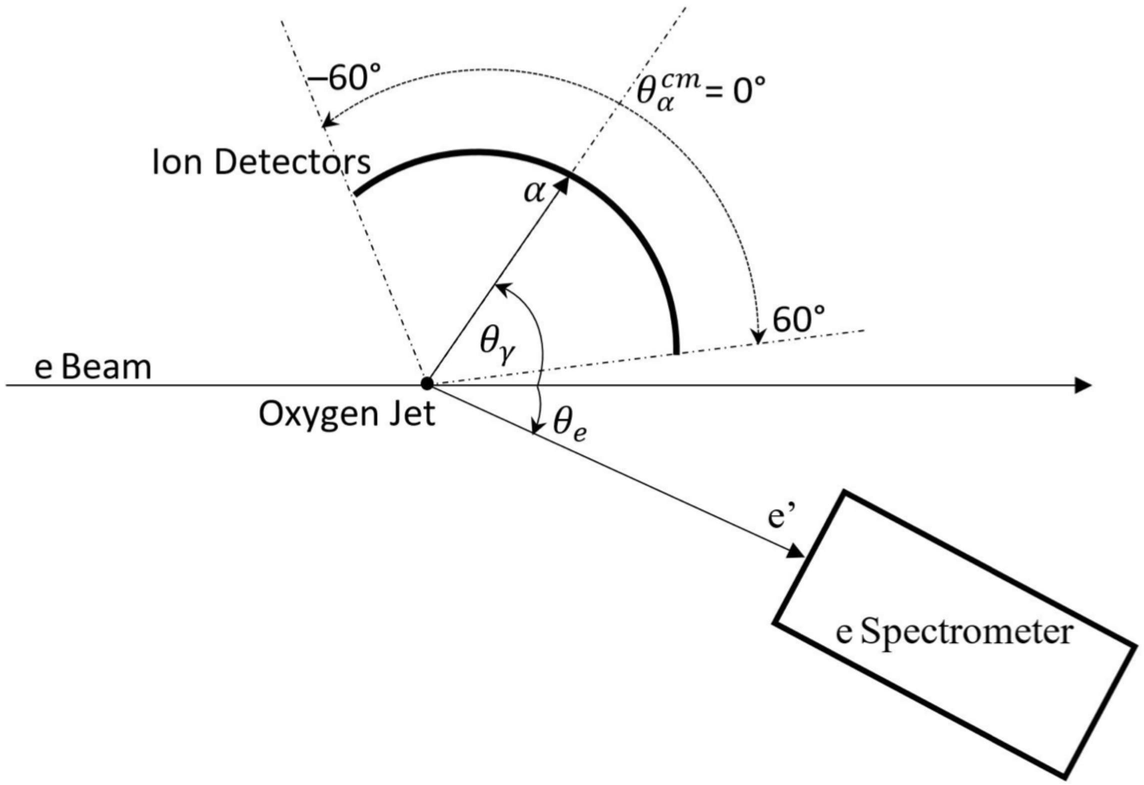

CBETA e-beam: 40 mA, E_0 = 78, 114, 150 MeV

Schematic layout of MAGIX approach

- Phase 0 and 1
- Phase 2

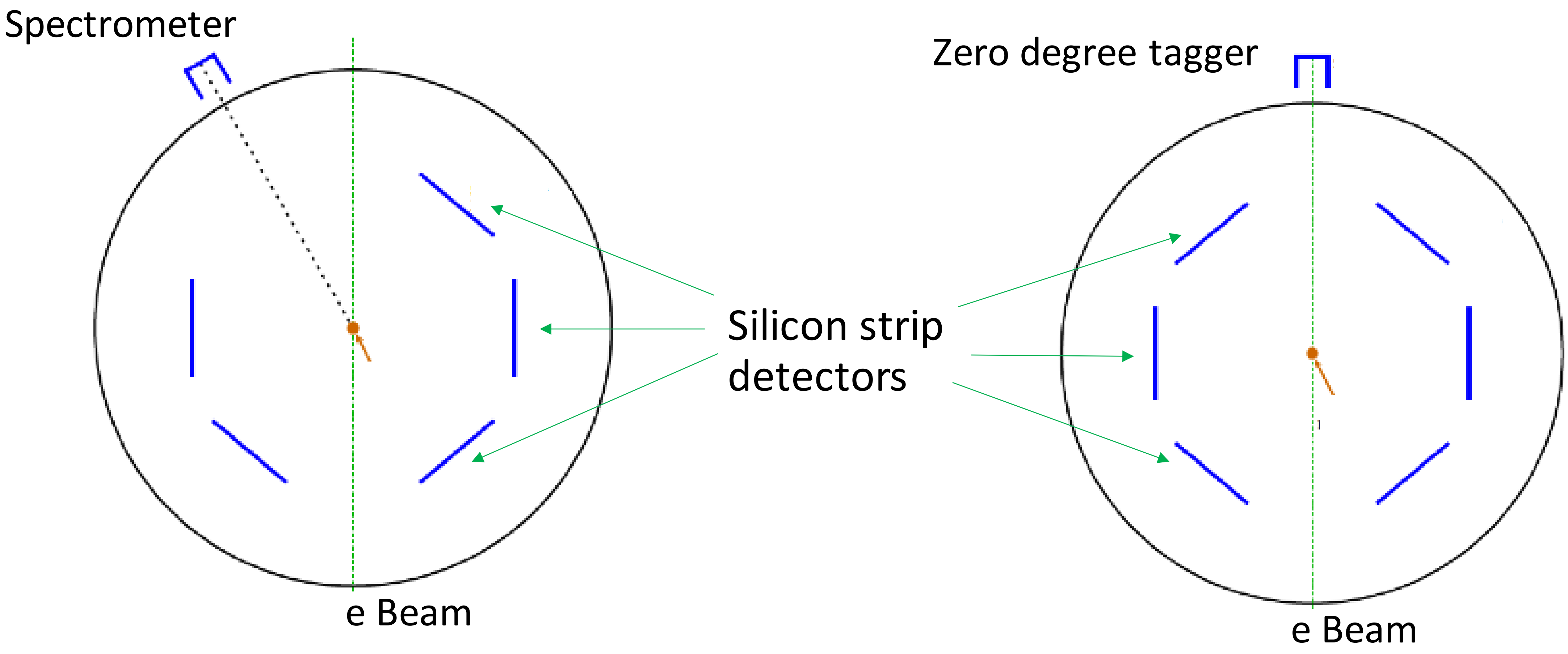

Systematics from oxygen isotopes

- Oxygen isotope abundance: ^{16}O 99.757%, ^{17}O 0.038% and ^{18}O 0.205%

K. J. R. Rosman, P. D. P. Taylor, Pure Appl. Chem 71 (1999) 1593

$$Q(^{16}O \rightarrow \alpha + {}^{12}C) = -7.162\ \text{MeV}$$
$$Q(^{17}O \rightarrow \alpha + {}^{13}C) = -6.359\ \text{MeV}$$
$$Q(^{18}O \rightarrow \alpha + {}^{14}C) = -6.228\ \text{MeV}$$

- Photonuclear cross sections:

natural abundance of O isotopes + depletion of ^{17}O and ^{18}O by factor 1000, and 5 ppmv for ^{14}N

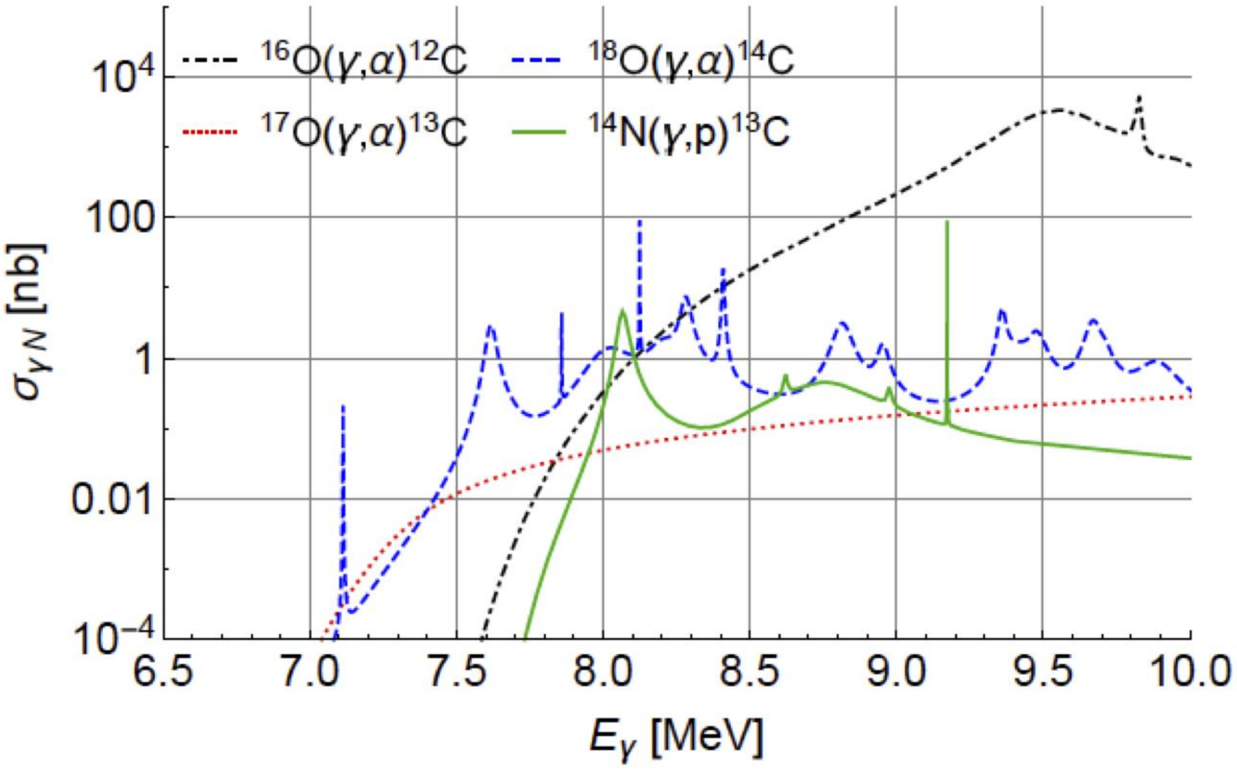

https://wiki.jlab.org/ciswiki/index.php/Simulations_and_Backgrounds#Relevant_Theoretical_Cross_Sections

Systematics from oxygen isotopes: Solution

- SRIM simulation: energy loss of α-particles in 2 mm wide oxygen jet, with a density of $6.65 \cdot 10^{-4}$ g/cm^3, E_e= 114 MeV, θ_e=15°, 1.0 ≤ E_α^{cm}≤1.1 MeV

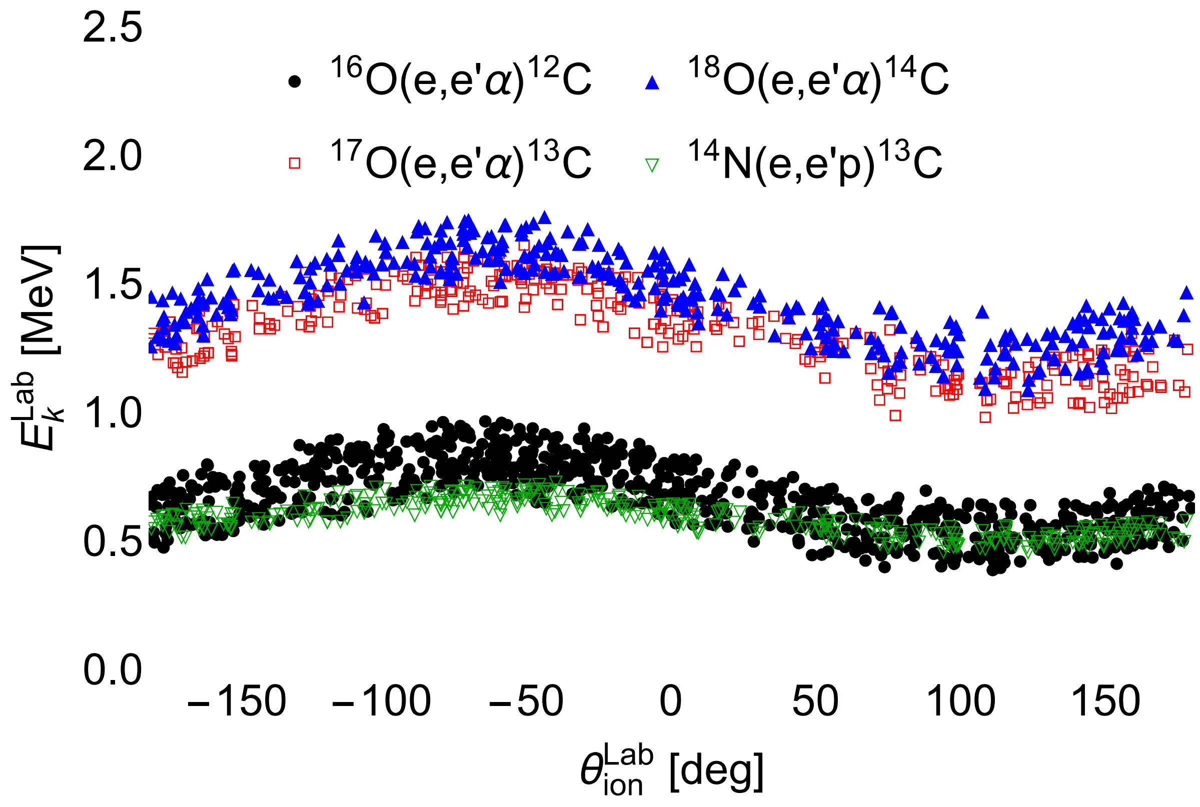

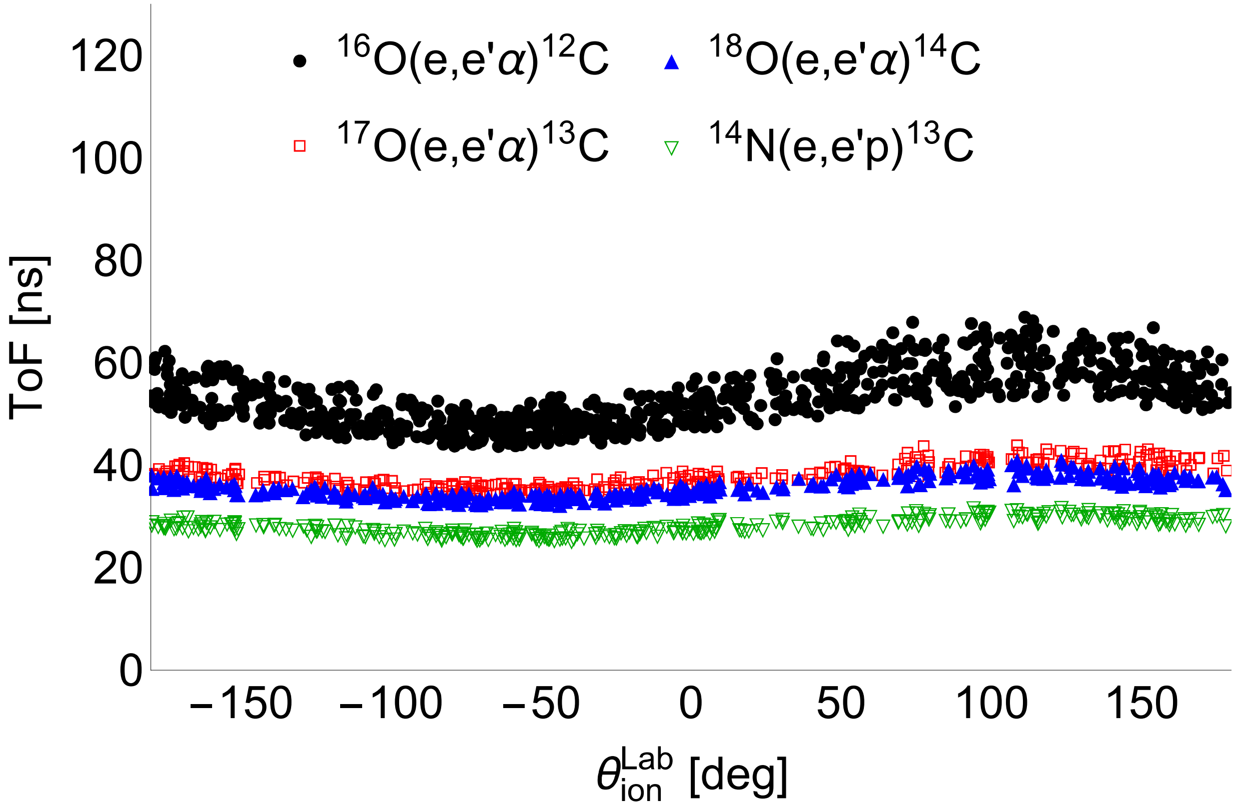

Virtual photon advantage

- SRIM simulation: angular spread of α-particles in 2 mm wide oxygen jet, with a density of $6.65{\cdot}10^{-4}$ g/cm^3, E_e= 114 MeV, θ_e=15° and 35°, $1.0 \leq E_\alpha^{cm} \leq 1.1$ MeV

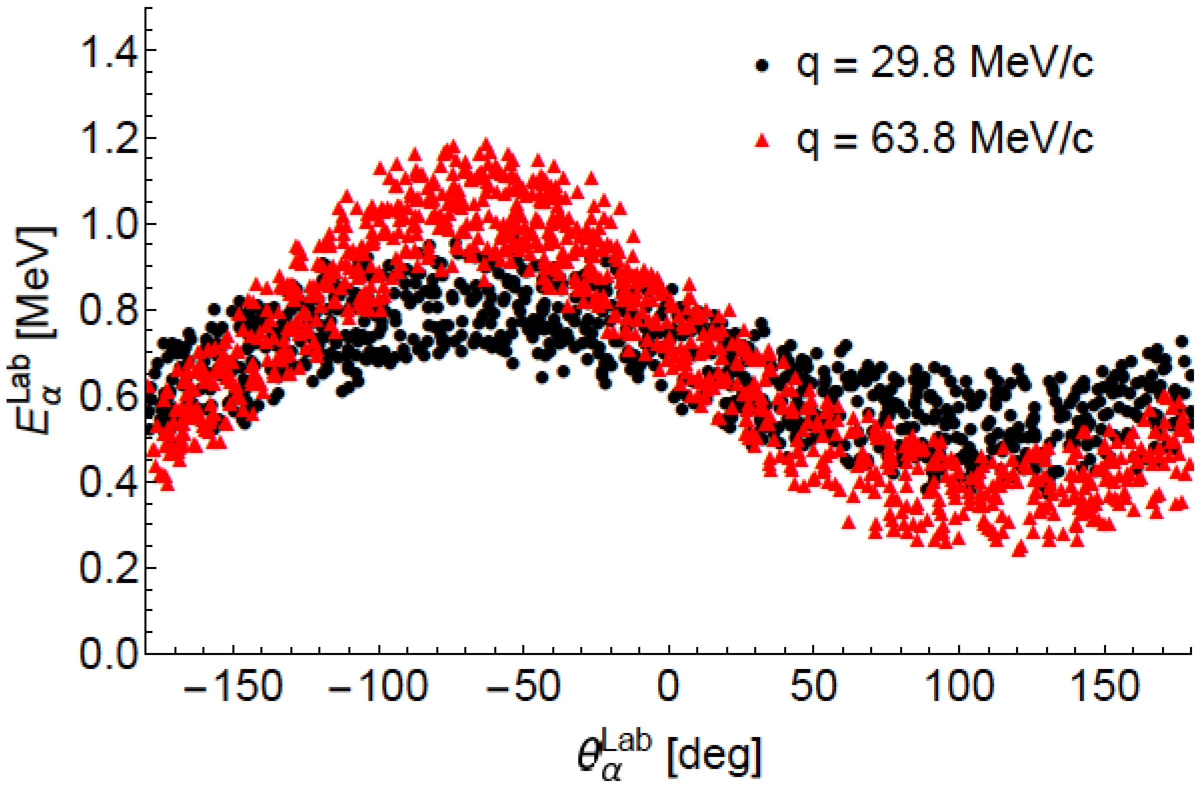

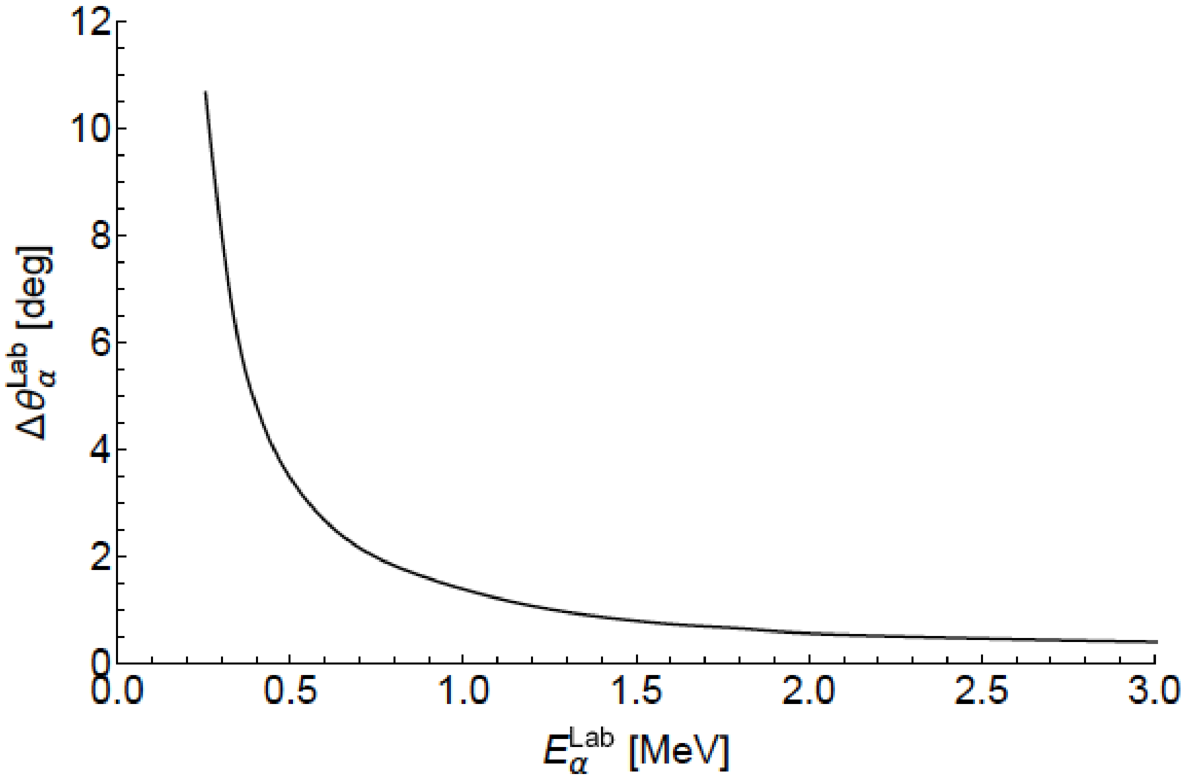

The cross section formulas

- Electrodisintegration of ^{16}O:

$$\frac{d\sigma}{dE'_e d\Omega_e d\Omega_\alpha^{cm}} = \frac{M_\alpha M_{12C}}{8\pi^3 W} \frac{p_\alpha^{cm}}{(\hbar c)^3} \sigma_{Mott} (\tilde{v}_L R_L + \tilde{v}_T \boldsymbol{R_T} + \tilde{v}_{LT} R_{LT} + \tilde{v}_{TT} R_{TT})$$

A. S. Raskin and T. W. Donnelly, Ann. of Phys. 191 (1989)

- Direct reaction $^{12}C(\alpha, \gamma)^{16}O$:

$$\left.\frac{d\sigma}{d\Omega_\gamma^{cm}}\right|_{(\alpha,\gamma)} = \frac{M_\alpha M_{12C}}{2\pi W} \frac{E_\gamma}{\hbar c} \frac{\alpha}{p_\alpha^{cm}} \boldsymbol{R}_{\boldsymbol{T},(\alpha,\gamma)}$$

$\tilde{v}_k$ lepton kinematic factors

R_k response functions

$\boldsymbol{R}_{\boldsymbol{T},(\alpha,\gamma)} = \boldsymbol{R_T}$ in real photon limit

Response functions for $J^{\pi} = 0^{+}$ nuclei

$$R_L = P_0(\cos\theta_\alpha)\left(|t_{C0}|^2 + |t_{C1}|^2 + |t_{C2}|^2\right)$$
$$+ P_1(\cos\theta_\alpha)\left(2\sqrt{3}|t_{C0}||t_{C1}|\cos(\delta_{C1} - \delta_{C0}) + 4\sqrt{\frac{3}{5}}|t_{C1}||t_{C2}|\cos(\delta_{C2} - \delta_{C1})\right)$$
$$+ P_2(\cos\theta_\alpha)\left(2|t_{C1}|^2 + \frac{10}{7}|t_{C2}|^2 + 2\sqrt{5}|t_{C0}||t_{C2}|\cos(\delta_{C2} - \delta_{C0})\right)$$
$$+ P_3(\cos\theta_\alpha)\left(6\sqrt{\frac{3}{5}}|t_{C1}||t_{C2}|\cos(\delta_{C2} - \delta_{C1})\right)$$
$$+ P_4(\cos\theta_\alpha)\left(\frac{18}{7}|t_{C2}|^2\right)$$

$$R_T = P_0(\cos\theta_\alpha)\left(|t_{E1}|^2 + |t_{E2}|^2\right)$$
$$+ P_1(\cos\theta_\alpha)\left(\frac{6}{\sqrt{5}}|t_{E1}||t_{E2}|\cos(\delta_{E2} - \delta_{E1})\right)$$
$$+ P_2(\cos\theta_\alpha)\left(-|t_{E1}|^2 + \frac{5}{7}|t_{E2}|^2\right)$$
$$+ P_3(\cos\theta_\alpha)\left(-\frac{6}{\sqrt{5}}|t_{E1}||t_{E2}|\cos(\delta_{E2} - \delta_{E1})\right)$$
$$+ P_4(\cos\theta_\alpha)\left(-\frac{12}{7}|t_{E2}|^2\right)$$

$$R_{TT} = -R_T\cos(2\phi_\alpha)$$

Matrix elements and coefficients

- Multipole matrix elements (q_0 = 1.2 fm^{-1}):

$$t_{EJ} = \frac{\omega}{q}\left(\frac{q}{q_0}\right)^J a'_{EJ}\left[1+\left(\frac{q}{q_0}\right)^2 b'_{EJ}(q)\right]e^{-\left(\frac{q}{q_0}\right)^2} \qquad t_{CJ} = \left(\frac{q}{q_0}\right)^J a'_{CJ}\left[1+\left(\frac{q}{q_0}\right)^2 b'_{CJ}(q)\right]e^{-\left(\frac{q}{q_0}\right)^2}$$

(t_{C0} leading dependence cannot occur due to orthogonality of initial and final state)

- Long wavelength limit and continuity equation:

$$t_{EJ} \to -\sqrt{\frac{J+1}{J}}\left(\frac{\omega}{q}\right)t_{CJ} \qquad a'_{EJ} = -\sqrt{\frac{J+1}{J}}\,a'_{CJ}$$

Leading order coefficients

- Second order polynomial fit to data $E_\alpha^{cm} < 1.7$ MeV

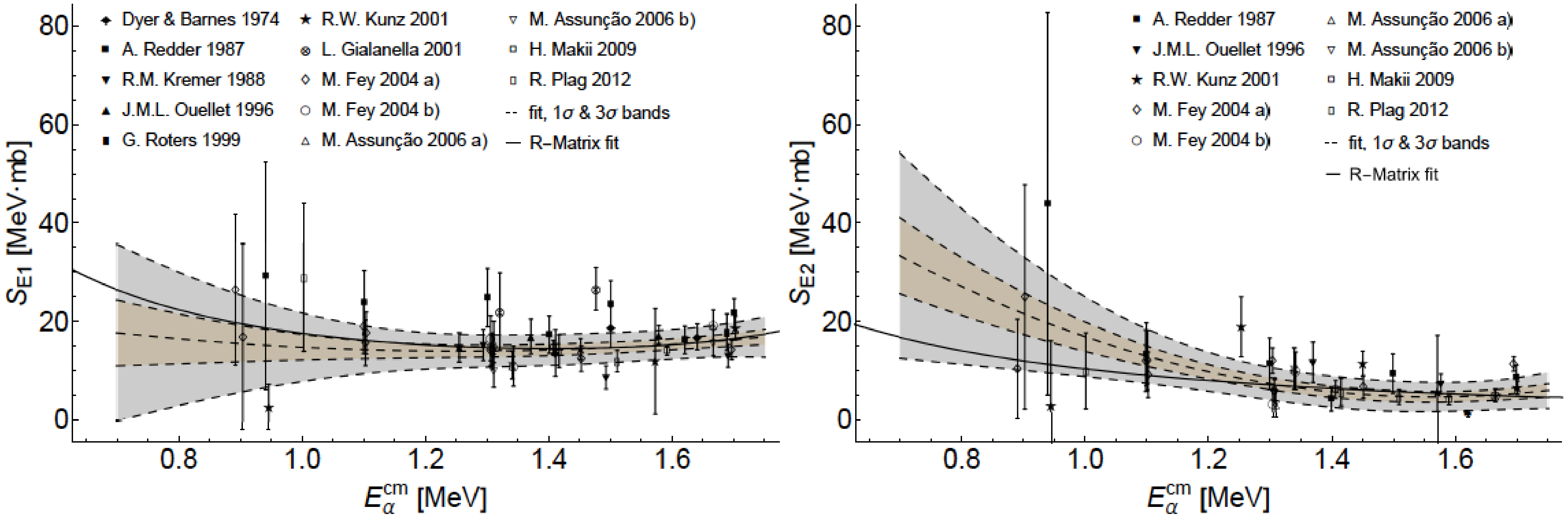

Next-to-leading order coefficients

- No knowledge about next to leading order coefficients $b'_{EJ,CJ}$ with $J = 1, 2$

  → Assuming $b'_{EJ,CJ} \approx 1$ and "+" sign
- No knowledge about C0 multipole and $b'_{C0} \cdot a'_{C0}$

  → Assuming $b'_{C0} \approx 1$ and "+" sign, **Case A** $a'_{C0} = a'_{E2}$ and **Case B** $a'_{C0} = 0.5a'_{E2}$
- For E_α^{cm}< 1.7 MeV only Coulomb phase contributes:

$$\delta_{Cl} - \delta_{C0} = \delta_{El} - \delta_{E0} = \sum_{n=1}^{l} \arctan \frac{\eta}{l}$$

Number of events after 100 days

- Events were sorted in:

→ four 1.91 MeV wide q-bins

→ ten 100 keV wide E_α^{cm}-bins

→ six 10° wide θ_α^{cm}-bins

- E_e= 114 MeV, θ_e=15°,

Case A and Case B

- **Now we can compute statistical uncertainties**

- Horizontal placement of data points according to:

G. D. Lafferty and T. R. Wyatt, Nucl. Instrum. Methods Phys. Res. A 355, 541 (1995).

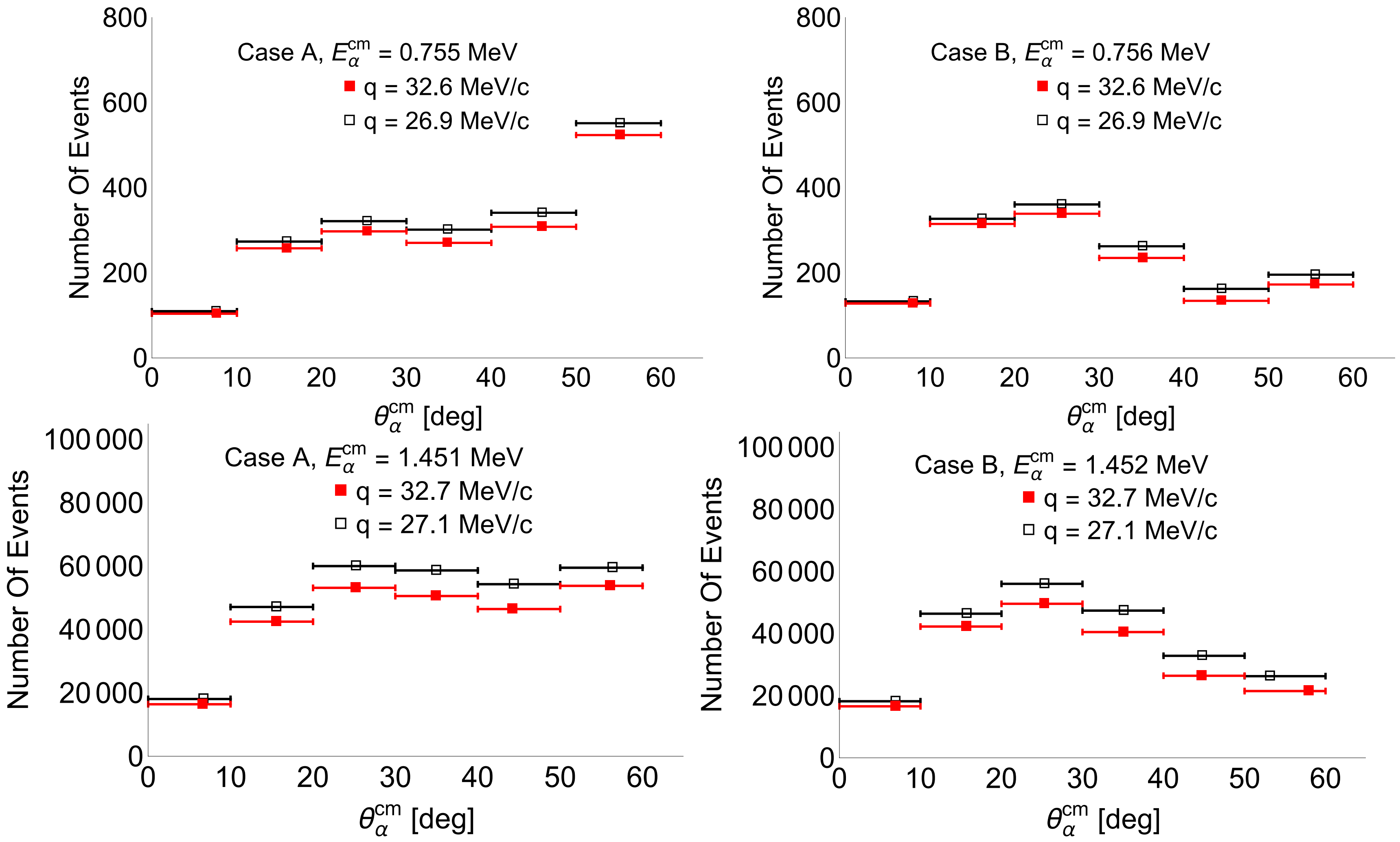

S-factors with projected statistical uncertainties

- E_e= 114 MeV, θ_e=15°, Case A and Case B
- Three fitting parameters a'_{E1}, a'_{E2} and a'_{C0} -> S_{E1}, S_{E2} and S_{aC0} non-astrophysical factor

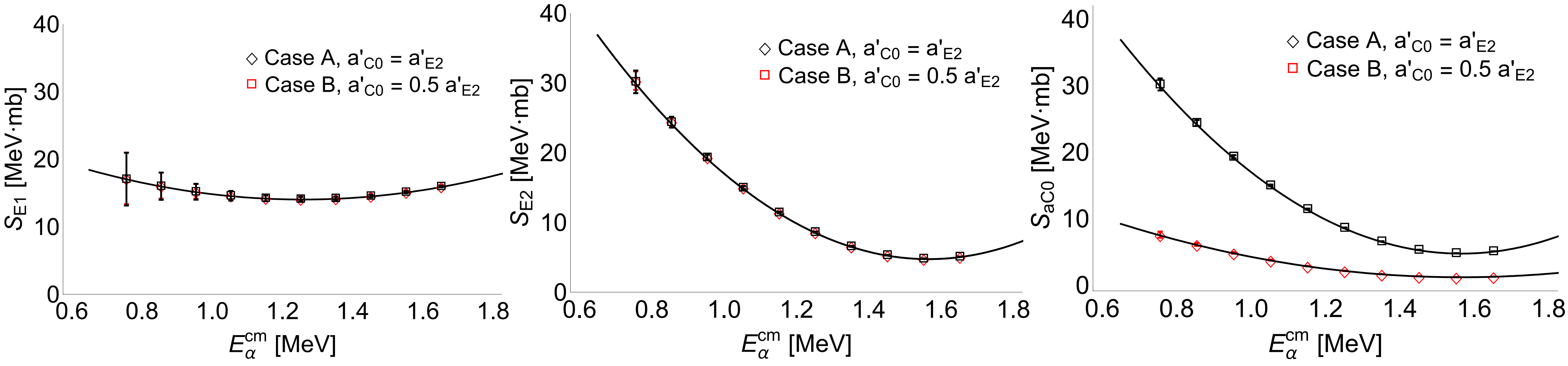

S-factors with projected statistical uncertainties

- E_e= 114 MeV, θ_e=15°, Case A

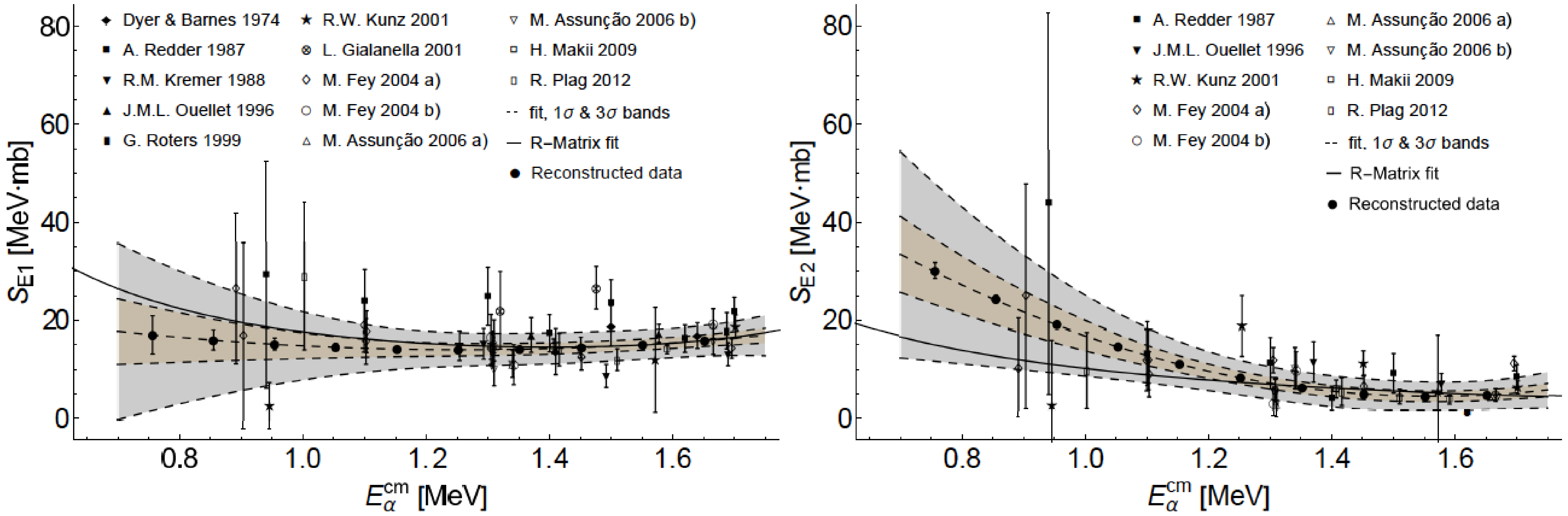

S-factors with projected statistical uncertainties

- E_e = 114 MeV, θ_e=15°, Case A
- Compared to most accurate measurements, statistical uncertainties of S_{E1} and S_{E2} are improved at least by factors 5.6 and 23.9, respectively

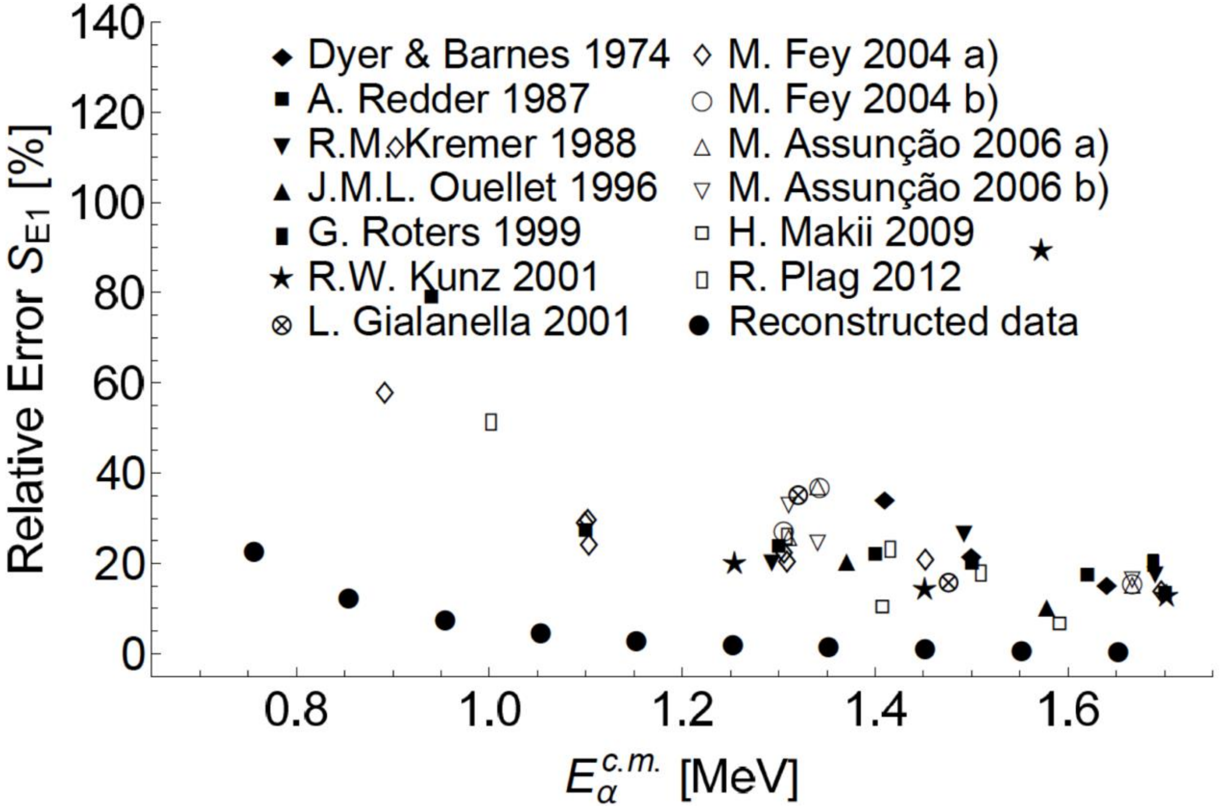

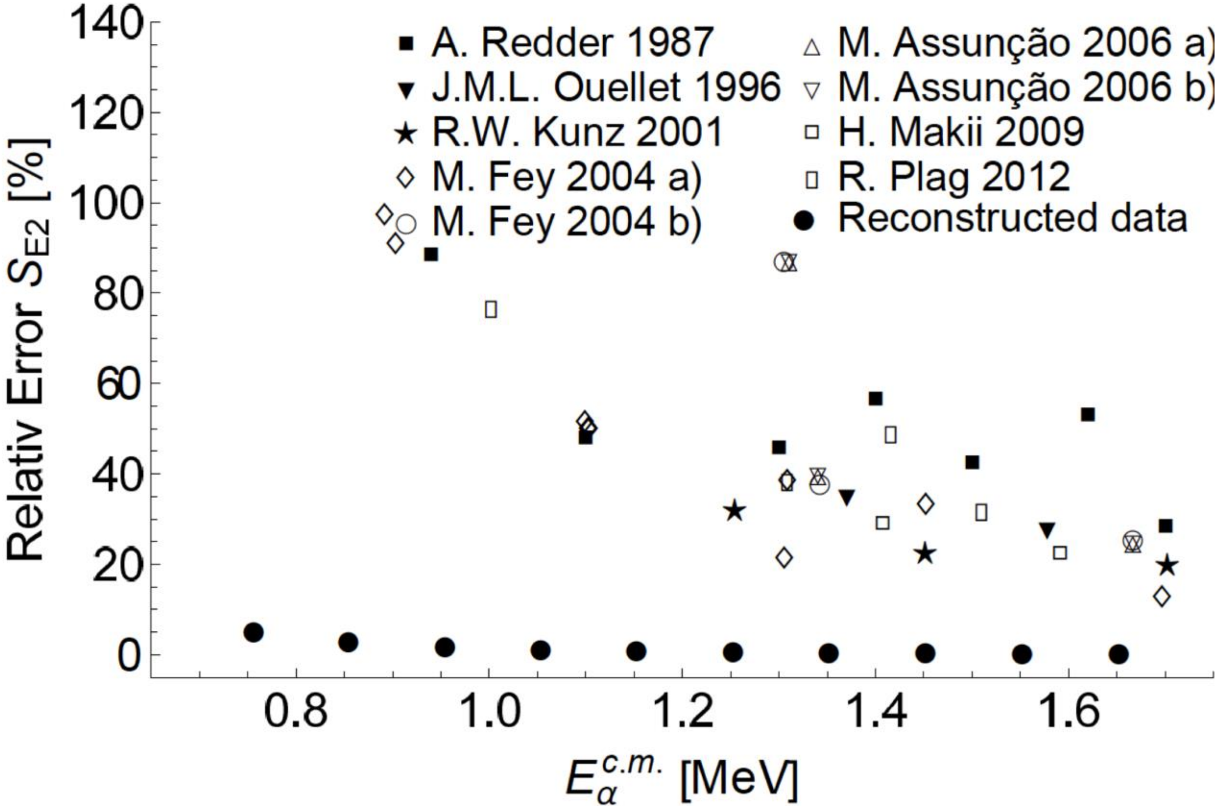

S-factors with projected statistical uncertainties

- E_e = 50 MeV, θ_e=15°, Case A, 10 mA for 100 Days
- E_e = 114 MeV, θ_e=15°, Case A, 10 mA for 100 Days

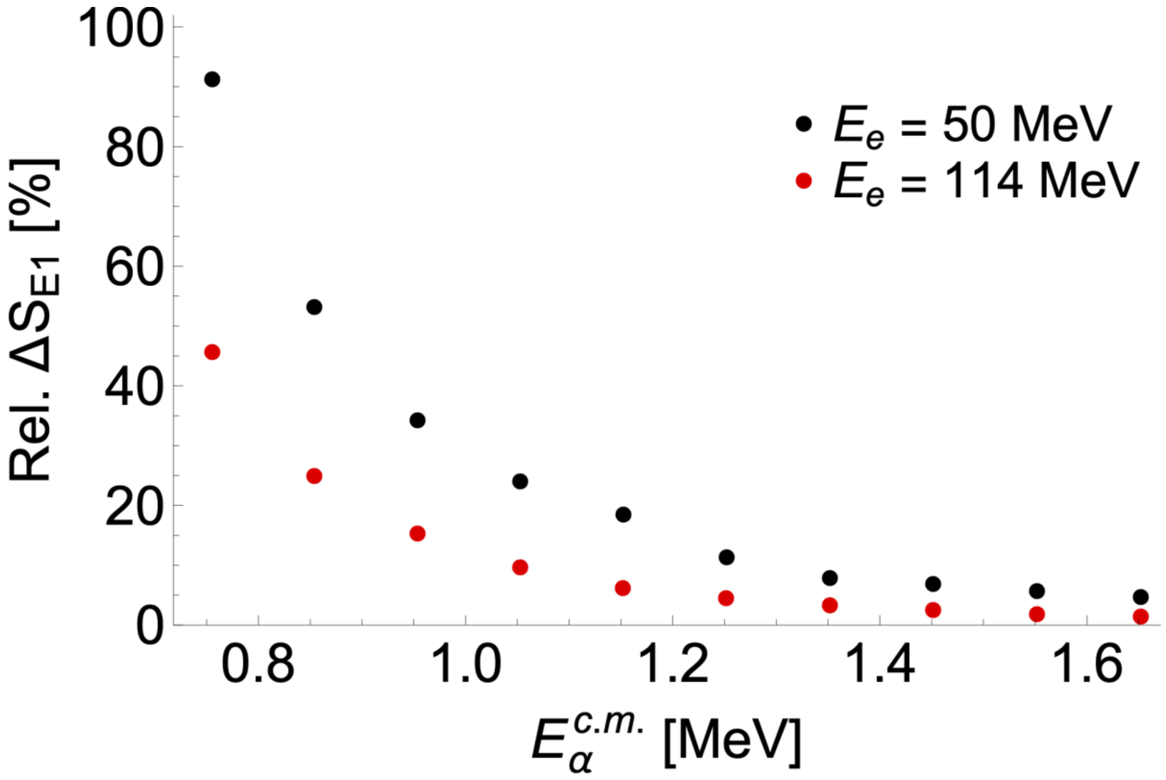

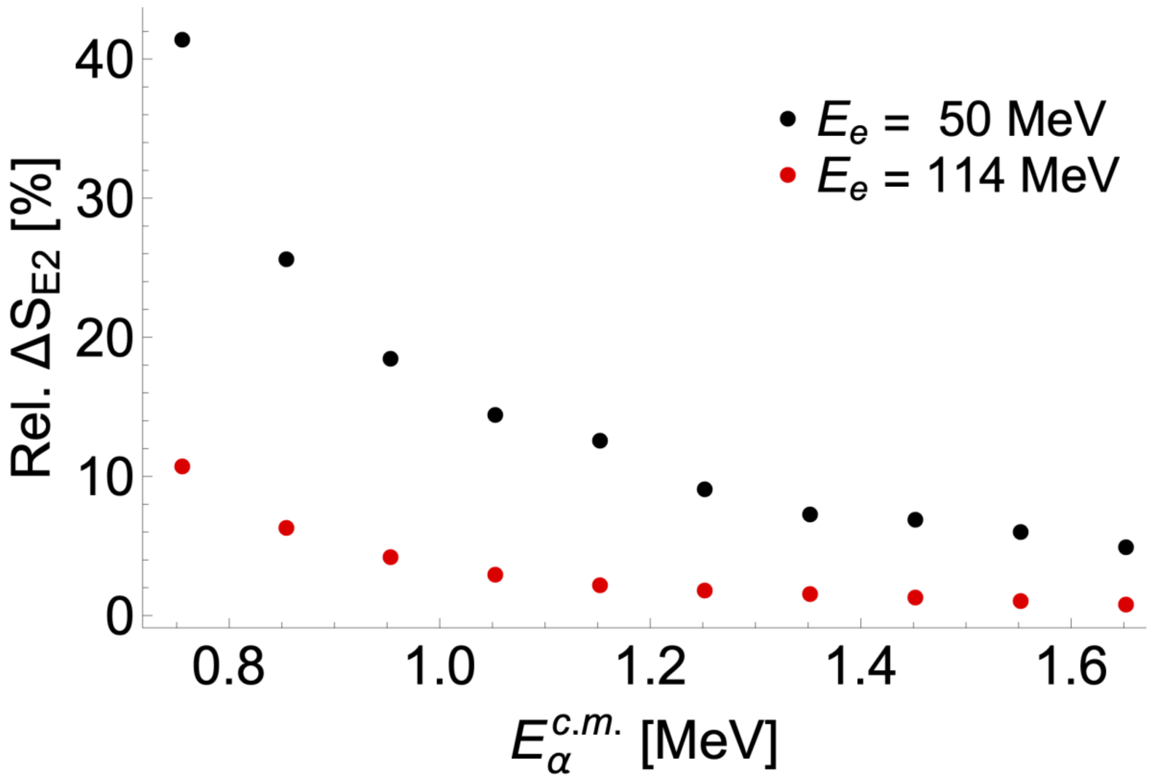

Conclusion

- Using a simple model, possibilities of new ERL accelerators and the gas-jet target, calculations of $^{16}O(e,e'\alpha)^{12}C$ reaction rate in range 0.7 < E_α^{cm} < 1.7 MeV and showed that one would be able to determine $^{12}C(\alpha, \gamma)^{16}O$ reaction rate with unprecedented statistical precision

- At E_e = 114 MeV and spectrometer with 10% E_e' acceptance the full range 0. < E_α^{cm} < 10.2 MeV is accessible from one experiment

- Shorter run at higher E_α^{cm} to test the particle identification (α from different Oxygen isotopes), systematics and all assumptions (next-to-leading order coefficients, q_0)

- For more details: **I. F.**, W. T. Donnelly and R. G. Milner, Phys. Rev. C 100, (2019) 025804

Currently supported by Croatian Science Foundation under the project IP-2018-01-8570 and European Union’s Horizon 2020 research and innovation program under the grant agreement 101038099.

Thank you